Physical mechanisms for hot-electron degradation in GaN light-emitting diodes

K. K. Leung,[1] W. K. Fong,[1] P. K. L. Chan,[2] and C. Surya[1,a)]
[1]*Department of Electronic and Information Engineering, The Hong Kong Polytechnic University, Hong Kong, People's Republic of China*
[2]*Department of Mechanical Engineering, The Hong Kong Polytechnic University, Hong Kong, People's Republic of China*

(Received 23 October 2009; accepted 3 February 2010; published online 5 April 2010)

We report investigations on the degradation of GaN-based light-emitting diodes due to high dc current stress by examining two types of devices with the same fabrication procedures except for the growth conditions for the InGaN quantum wells (QWs). Higher trimethylindium and triethylgallium fluxes are used for type A devices resulting in a threefold increase in the InGaN QWs growth rate compared to type B devices. Detailed structural and optoelectronic properties of the devices are investigated by transmission electron microscopy, atomic force microscopy, thermal imaging, *I-V* measurements, and the low-frequency noise properties of the devices as a function of the stress time, t_S. The experimental data show that the QWs in type B devices are dominated by spiral growth and they have substantially higher strain nonuniformity than type A devices. The highly strained GaN/InGaN interfaces in device B are also responsible for the faster increase in the defect density due to hot-electron injection. The defects enhance the trap-assisted tunneling in the multiple quantum wells (MQWs) resulting in the development of hot spots among type B devices after high current stressing of the MQWs. This in turn leads to an increase in the defect generation rate resulting in a thermal run-away condition that ultimately resulted in the failure of the device. The data show that an increase in the growth rate in the InGaN layer led to the domination by the step flow growth mode over the spiral growth mode in the MQWs. This is the main reason for the reduction in the dislocation density in type A devices and hence their increase in device reliability. © *2010 American Institute of Physics*. [doi:10.1063/1.3357312]

I. INTRODUCTION

III-nitrides are the materials of choice for the development of high-power light-emitting diodes (LEDs) and laser diodes.[1–5] Wide application of LEDs may potentially lead to ~50% savings in energy consumed for lighting purpose. Device reliability is an important issue especially for high-power applications. The lifetimes and reliability of the devices are closely correlated with the crystal quality of the semiconductor films.[6–8] The growth of high quality InGaN QWs required for high brightness and reliable devices is still a major challenge. This is mainly due to the large lattice mismatch between GaN and the sapphire substrate leading to high dislocation density in the GaN films with significant implications on the reliability and lifetimes of the devices.[9] Optimization of the InGaN QW growth process is critical for the enhancement of the optoelectronic properties and reliability of the LEDs.

The growth parameters of the InGaN QWs have significant impacts on the optoelectronic properties of the device. It has been shown that the incorporation efficiency of indium into the InGaN epitaxial layers is strongly dependent on the growth rates of the films. Work by Keller *et al.*[10] demonstrated that small variations in the growth rate of the InGaN layer may have significant impact on the growth mode of the materials. The step-flow growth mode competes with the spiral growth mode around threading dislocations with a screw component. It was found that the spiral growth mode may dominate under low growth rate conditions and substantial increases in the rms roughness of the films were observed with the reduction in triethylgallium (TEG) flow. The domination by spiral growth mode may result in large strain nonuniformity in the InGaN QWs[11] and it will significantly reduce the lifetime and efficiency of the device. The strain level in the InGaN layer must be carefully managed through optimizing the growth conditions as excessive strain will lead to the reduction in the local critical thickness of the InGaN layer and the formation of threading dislocations in the multiple quantum well (MQW).

The reliability of GaN-based LEDs has been a subject of interest to different research groups.[12,13] Understanding the physical mechanism underlying the degradation process is critical for optimizing the device structure and the enhancement of the device reliability. Furthermore, this can also form the basis for the development of a fast screening process for LEDs as the LED manufacturers typically spend up to thousands of hours in high current stressing of LEDs to determine the average lifetime of a particular batch of devices. Such process is time consuming and usually only a small percentage of devices will be tested. A fast screening process will be highly desirable for cost saving and to facilitate a higher percentage of devices to be tested within a batch.

[a)]Author to whom correspondence should be addressed. Electronic mail: ensurya@polyu.edu.hk.

 © 2010 American Institute of Physics

Downloaded 17 Mar 2011 to 158.132.161.180. Redistribution subject to AIP license or copyright; see http://jap.aip.org/about/rights_and_permissions

TABLE I. The growth conditions for type A and type B devices.

	Type A devices	Type B devices
InGaN well (3 nm)	TEG=10.56 μmol/min TMI=19.39 μmol/min TMI/(TMI+TEG)=64.7%	TEG=3.52 μmol/min TMI=13.96 μmol/min TMI/(TMI+TEG)=79.9%
GaN barrier (8 nm)	27.54 μmol/min	27.54 μmol/min

A number of authors had pointed out that hot-electron degradation of the devices is associated with the increase in the low-frequency excess noise of the device.[14–16] This is not surprising as the low-frequency excess noise of a semiconducting device has been shown to be directly proportional to the defect density in the material. It has been demonstrated that there is a strong correlation between the initial rate of increase in the low-frequency noise level and the lifetime of the device.[16] The decrease in the device lifetime is related to the increase in the defect density.[17] It is important to identify relationship between the degradation of the optoelectronic and low-frequency noise properties of the device to further elucidate on the phenomenon. In the current work, we performed detailed investigations on the degradation of the optoelectronic properties of GaN LEDs due to the application of a high dc stressing current.

II. EXPERIMENT

Gallium nitride epitaxial layers were grown on (0001) sapphire substrates using a Thomas Swan close-coupled showerhead metal organic chemical vapor deposition (MOCVD) reactor. A 30 nm thick GaN nucleation layer was deposited at 520 °C. This was followed by a 2 μm thick undoped GaN epilayer deposited at 1035 °C and a pressure of 200 Torr. Ditertiarybutyl silane was used as a dopant source for the growth of n-doped GaN[18–20] and the carrier concentration of the n-layer is 3×10^{18} cm^{-3}. The active region consists of a five-period GaN/InGaN MQW, where the InGaN QWs were grown at 700 °C and the GaN barriers at 850 °C. Finally, a 150 nm thick p-GaN layer of doping concentration $\sim4\times10^{17}$ cm^{-3} was grown at 1010 °C on top of the MQWs. High transmittance ITO and Ti/Al (10nm/10nm) layer were used for the p-type and n-type Ohmic contacts, respectively.[21–24] To identify the physical origin of the degradation of the LEDs, detailed characterizations including structural, optoelectronic, low-frequency noise and thermal imaging measurements were performed on the devices as a function of the stress time and the results are compared and discussed. Two different types of devices were being examined which had undergone the same fabrication procedures except for the growth conditions of the QWs as indicated in Table I. For type A devices the TEG and trimethylindium (TMI) fluxes were 10.56 μmol/min and 19.39 μmol/min compared to 3.52 μmol/min and 13.96 μmol/min, respectively, for type B devices. The growth rate for the InGaN QWs in type A devices is roughly three times faster than that for type B devices.

III. RESULTS AND DISCUSSION

A. Morphological characterization of active region

The transmission electron microscopy (TEM) pictures of the MQWs for type A and B devices are shown in Figs. 1(a) and 1(b), respectively. It is observed that type B device exhibits substantially higher nonuniformity in the MQW structure with significant out-diffusion of indium. It is believed that indium out-diffusion is associated with the presence of threading dislocations in GaN films.[25,26] A low InGaN growth rate used in type B devices resulted in the domination by the spiral growth mode leading to an increase in the interface roughness as well as the building up of uneven strain in the MQWs. If the local strain becomes excessive threading dislocations may develop to facilitate the relaxation of strain in the MQWs. This corroborates with the experimental results on atomic force microscopy (AFM) scanning of the QW layers in Fig. 2 which shows 40% increase in the dislo-

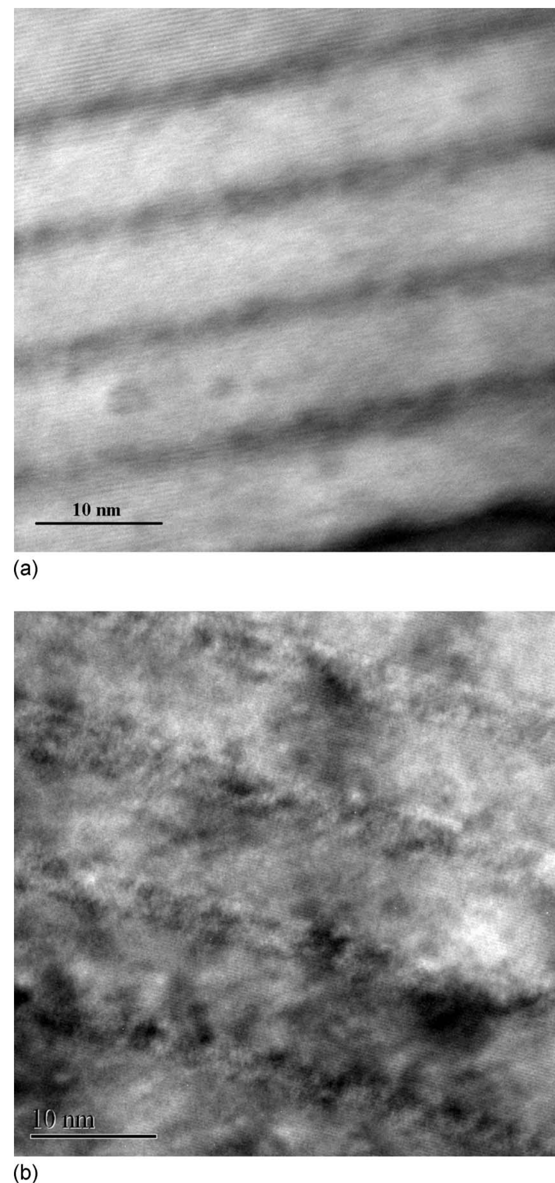

FIG. 1. TEM pictures of (a) type A device; (b) type B devices before current stressing.

Downloaded 17 Mar 2011 to 158.132.161.180. Redistribution subject to AIP license or copyright; see http://jap.aip.org/about/rights_and_permissions

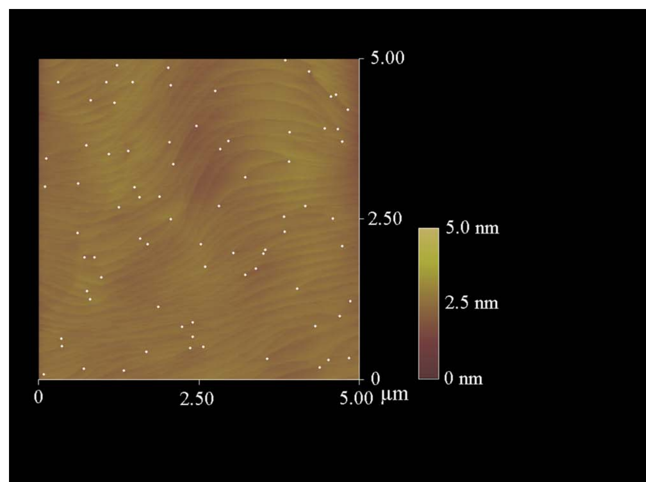

(a)

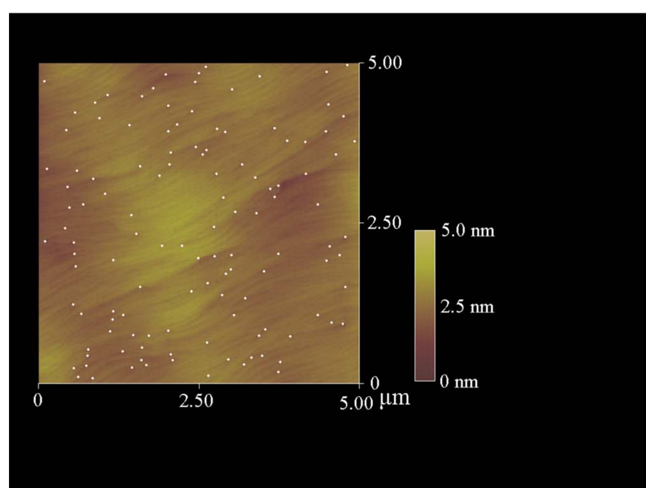

(b)

FIG. 2. (Color online) AFM pictures of (a) type A; (b) type B devices. The positions for threading dislocations are indicated by the white dots.

cation density for type B samples. It can also be noticed that the threading dislocation density increases with the surface roughness of the devices.

B. Characterization of electrical properties

The *I-V* characteristics for the devices were characterized under different stressing times (t_S) using a dc stressing current density of 60 A cm^{-2}. After 24 h of accelerated stressing, the devices exhibit significant increases in the reverse bias saturation currents as well as current bumps in the forward *I-V* curves. Both type A and type B devices exhibit similar characteristics for t_S=0 and 24 h as shown in Fig. 3. The increase in the device current both under forward and reverse bias is believed to arise from the increases of the defect-assisted tunneling in the MQWs.

C. Characterization of optical properties

Figure 4 illustrates the experimental electroluminescence (EL) for both types of devices. The data demonstrate similar EL peaks for both devices indicating that high InGaN growth rate enhances In incorporation in the QWs. It is also noted

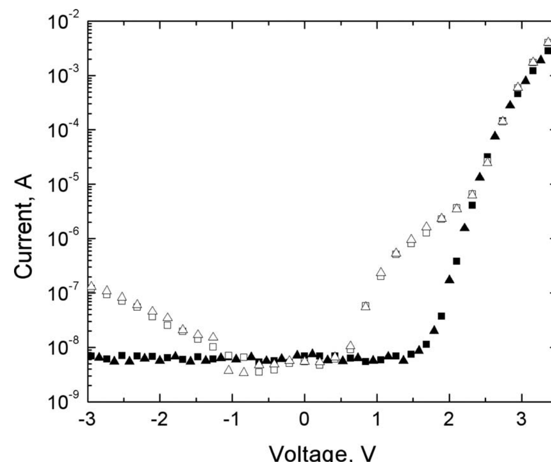

FIG. 3. Typical IV measurement of type A devices before stressing at t_S =0 h (solid triangle) and after stressing at t_S=24 h (open triangle); and type B devices before stressing at t_S=0 h (solid square) and after stressing at t_S=24 h (open square).

that although the MQWs were grown using N_2 as the carrier gas, small amount of hydrogen may be generated from the cracking of NH_3 which may cause preferential etching of In at the growth surface. A slow growth rate may amplify this effect leading to nonuniformity in the QWs. Furthermore, over 30% increase in the internal quantum efficiency was observed for device A. After the devices were stressed by constant current, both devices show substantial drop in the EL which indicates the generation of nonradiative defects in the MQWs.

D. Characterization of low-frequency noise properties

The hot-electron degradation of the optoelectronic properties of the devices are consistent with the generation of localized states in the MQWs. The trap density is characterized by the examination of the low-frequency noise power spectral density of the device. Noise measurement as a characterization tool has important advantages over many conventional techniques because it is nondestructive and it can be performed directly on the device itself. It has been shown

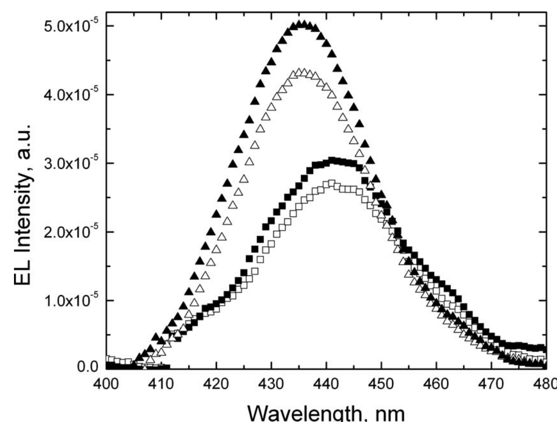

FIG. 4. Typical EL measurement of type A devices before stressing at t_S =0 h (solid triangle) and after stressing at t_S=24 h (open triangle); and type B devices before stressing at t_S=0 h (solid square) and after stressing at t_S=24 h (open square).

Downloaded 17 Mar 2011 to 158.132.161.180. Redistribution subject to AIP license or copyright; see http://jap.aip.org/about/rights_and_permissions

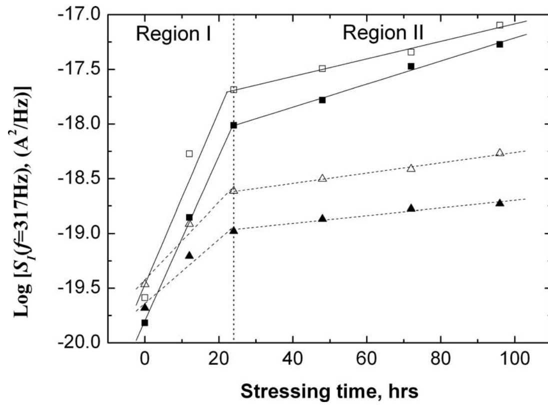

FIG. 5. Experimental data on $S_I(f)$ against stressing time for type A (open and solid triangle) and B (open and solid square) devices.

that conductance fluctuations in MQWs device arise from the modulation of the tunneling barrier due to the capture of a carrier by a localized state in the barrier layer. This leads to a fluctuation in the device current when a constant voltage is applied to the structure. The current noise power spectral density is given by[27]

$$S_I(f) = 4(\Delta I_0)^2 \int_E \int_z \int_y \int_x N_T(E) \frac{\tau}{1+4\pi^2 f^2 \tau^2} dxdydzdE, \quad (1)$$

where ΔI_0 is the current fluctuation in the device due to the capture of a single carrier by a localized state, $N_T(E)$ is the trap density in the material and τ is the time constant of the fluctuation process. Previous studies showed that τ is thermally activated and can be expressed as[28]

$$\tau = \tau_0 \exp\left(\frac{E}{k_B T}\right), \quad (2)$$

where E is the activation energy of the localized state, k_B is the Boltzmann constant and T is the absolute temperature. The Lorentzian in Eq. (1) is a sharply peaked function of E. Thus, $S_I(f)$ is highly sensitive to the traps at $E_p = -k_B T \ln(\tau_0 \omega)$ where E_P is the energy where the Lorentzian peaks. Based on Eq. (1) a normalized trap density, $N_{TR}(E)$, can be defined as

$$N_{TR}(E_p) \approx \frac{4Cf}{k_B T} S_I(f,T), \quad (3)$$

in which C is a proportionality constant. Equation (3) shows that $S_I(f)$ is proportional to the trap density at E_P. The experimental data on the low-frequency noise measurements are shown in Fig. 5. The current noise power spectra, $S_I(f)$, were found to increase as a function of t_S. From Fig. 5 one observes that $S_I(f)$ can be roughly divided into two regions: in region I ($t_S < 24$ h), devices demonstrate high rates of increase in $S_I(f)$ with t_S; in region II ($t_S > 24$ h), the rates of increase in $S_I(f)$ are found to be substantially lower than in region I. It is also observed that type B devices show close to two orders of magnitude increase in $S_I(f)$ in region I compared to about sixfold increase in $S_I(f)$ for type A devices in the same region. This stipulates close to two orders of magnitudes increase in $N_{TR}(E)$ for device B in region I, whereas only about sixfolds of increase in $N_{TR}(E)$ is observed for the type A device over the same region. In region II, both types of devices exhibit much lower rates of increase in $N_{TR}(E_P)$ than in region I. This phenomenon can be explained based on the differences in the material strain in the QWs. The significant increase in defect density for the type B device in region I is attributed to the presence of highly strained bonds at the MQWs which may be easily broken at the application of a stressing current resulting in the generation of a large quantity of localized states. However, once the strained bonds were broken, the MQWs would become more stable and the rate of increase in the trap density at the MQWs would be substantially lowered as shown in Fig. 5. It is noted that the rate of increase in trap density for the type B devices in region II remains somewhat higher than the type A devices. This can be accounted for by the presence hot spots in the MQWs for the type B devices. The generation of defect states is a thermally activated process, an elevation in the temperature will lead to a higher generation rate for the defects. It is noteworthy that the experimental results agree with the observations by Ursutiu and Jones[16] that an inverse correlation exists between the initial rate of increase in the low-frequency noise and the lifetime of the LED. The model provides a physical basis for the observation that devices with high initial rate of increase in the low-frequency excess noise generally also exhibit shorter lifetimes due to hot-electron stressing. Thus, the measurement of low-frequency noise can be utilized as a cost-effective screening technique for LEDs.

E. Thermal reflectance measurement

It is important to identify the position of the defects generated in the device to determine the detailed failure mechanism. Based on the model presented above the defects generated in the stressing experiment would be physically correlated with the high current regions of the device which can be effectively investigated by systematic thermal imaging of the devices under high dc current stress. The temperature differentials of the devices over the entire surface area were determined by CCD-based thermoreflectance. Local variation in the temperature of the device will lead to corresponding changes in the reflectance, R, given by[29]

$$R(T) = R(T_0) + \frac{\partial R}{\partial T}(T - T_0), \quad (4)$$

and the temperature differential can be evaluated by

$$\Delta T = \frac{1}{\beta} \frac{\Delta R}{R(T_0)}, \quad (5)$$

where $\Delta T = T - T_0$ and β is the thermal reflectance coefficient and is given by $\beta = \partial R / \partial T [1/R(T_0)]$.[30] The results obtained for both types of devices under a dc current bias of 100 mA, prior to the application of an accelerated stressing current, are shown in Fig. 6. In contrast to the hot spots being developed in the type B device, type A device shows a much more uniform temperature distribution over the entire device surface. To examine the effects of hot-electron injection on the

Downloaded 17 Mar 2011 to 158.132.161.180. Redistribution subject to AIP license or copyright; see http://jap.aip.org/about/rights_and_permissions

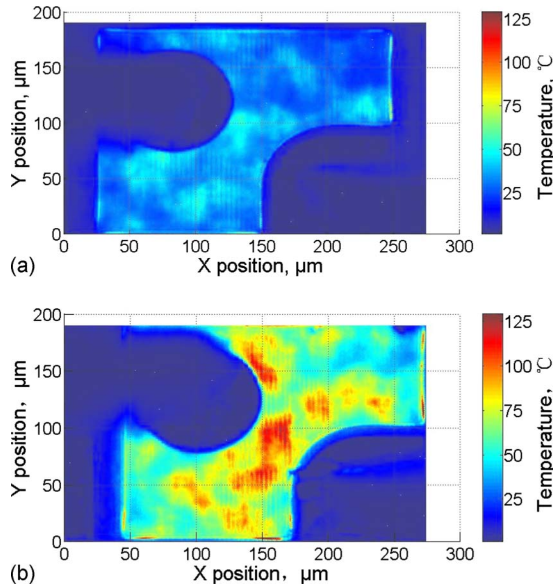

FIG. 6. (Color online) Temperature profile of top view of (a) type A; (b) type B devices before stressing.

temperature distribution, the two devices were subjected to a high stressing current of 600 A cm^{-2} for a period of 24 h and the thermal images of the devices were again measured under a biasing current of 60 mA as shown in Fig. 7(a). Higher nonuniformity in the thermal image is observed in device A while for device B, a large dark spot has been developed over the region where the hot spots were observed in Fig. 7(b). The overall brightness of device B has been substantially reduced which is related to the total failure of the device. It is noted that it takes 6 days of continued high current stressing at 600 A cm^{-2} for device A to reach a similar condition for the dark spot to be observed as in device B.

F. Materials defects and hot-electron hardness

The TEM images of the samples are shown in Fig. 8. While device A demonstrate an intact MQW after 24 h of

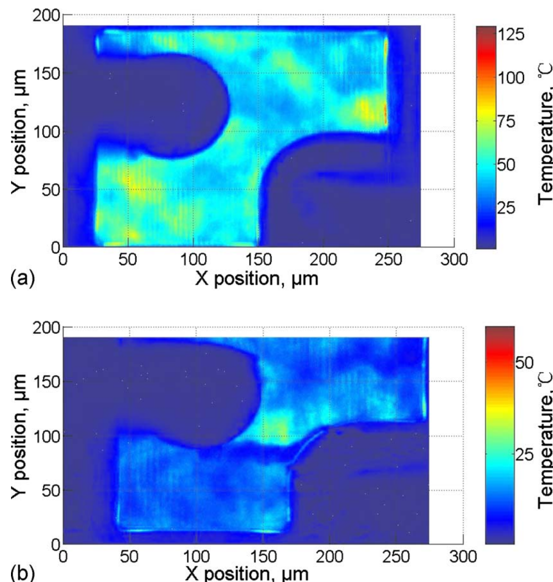

FIG. 7. (Color online) Temperature profile of top view of (a) type A; (b) type B device after 24 h high current stressing. The periodic noise is due to the diffraction of the optical filter.

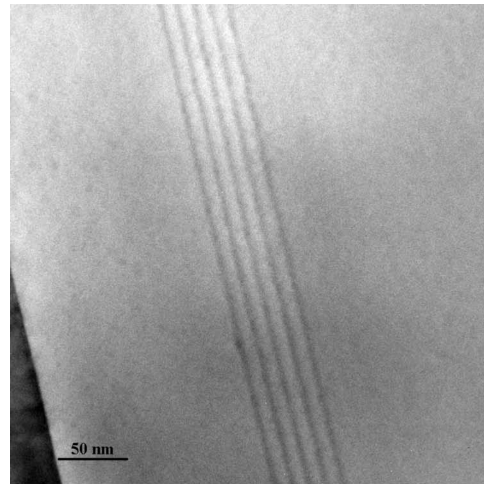

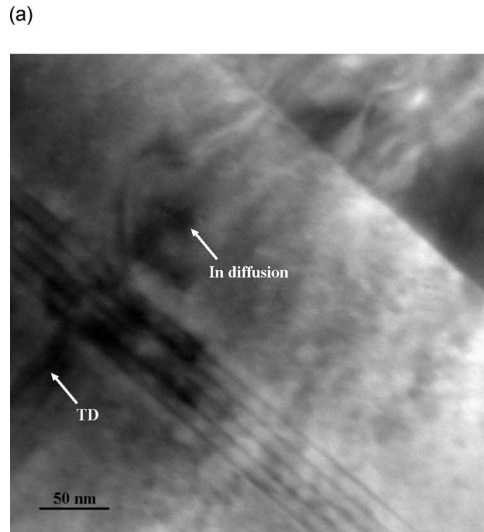

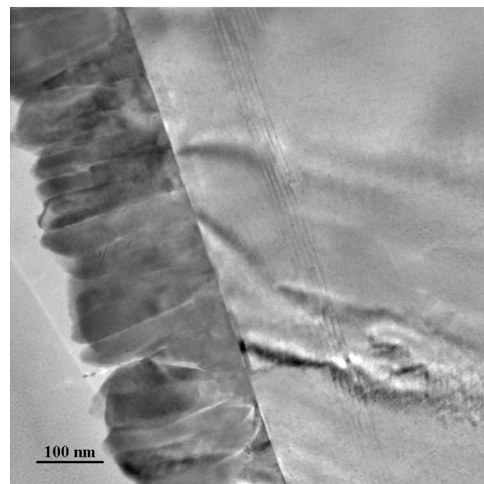

FIG. 8. TEM pictures of (a) type A device after 24 h high current stressing; (b) type B device after 24 h high current stressing; and (c) type A device after 144 h high current stressing.

high current stress as shown in Fig. 8(a), substantial indium out-diffusion is seen in a failed device B for $t_S=24$ h as indicated in Fig. 8(b). Moreover, one can clearly see, from the figure that, a threading dislocation has been developed originating from the MQW and similar observation was

Downloaded 17 Mar 2011 to 158.132.161.180. Redistribution subject to AIP license or copyright; see http://jap.aip.org/about/rights_and_permissions

made on a failed type A device after six days of high current stress as indicated in Fig. 8(c). The data clearly show that high dc current stressing over extended period of time results in significant compromise in the structural integrity of the MQWs. Significant increase in the defect density such as localized states and threading dislocations have been observed in the MQWs.

IV. CONCLUSION

In conclusion, we have conducted systematic investigations on the degradation of the optoelectronic and low-frequency noise properties of GaN LEDs due to the application of a high dc stressing current. The experimental results indicate that significant increase in the defect density arise from hot-electron injection. Devices that were grown with a low growth rate for the InGaN quantum wells (QWs) (type B) were found to have high rates of degradation of the optoelectronic properties due to the high rate of generation of material defects. This is attributed to the domination of spiral growth in the QWs resulting in high strain nonuniformity. It was shown that the generation of defects led to an increase in the trap-assisted tunneling current resulting in the development of hot spots in the devices. This will further enhance the defect generation resulting in a thermal run-away condition which eventually resulted in the failure of the device.

It is noteworthy that high initial rate of increase in the low-frequency excess noise stipulates high strain in the MQWs. The highly strained bonds in the MQWs are more readily broken at the application of a high stressing current. This accounts for the observed shorter lifetimes for the type B devices. Our results provide the physical basis for the utilization of low-frequency noise measurement as a tool for the projection of the lifetimes of the devices.

ACKNOWLEDGMENTS

This work is supported in part by a grant from the Innovative Technology Commission under the Guangdong/Hong Kong Scheme (Project No. GHP/031/07GD) and an RGC Grant (Grant No. PolyU 5112/08E). Further support is provided by a Niche area grant of the Hong Kong Polytechnic University.

[1]S. Nakamura, T. Mukai, and M. Senoh, Appl. Phys. Lett. **64**, 1687 (1994).
[2]T. Kuroda and A. Tackeuchi, J. Appl. Phys. **92**, 3071 (2002).
[3]S. Nakamura, T. Mukai, and M. Senoh, Jpn. J. Appl. Phys., Part 1 **30**, L1998 (1991).
[4]S. Nakamura, M. Senoh, S. Nagahama, N. Iwasa, T. Yamada, T. Matsushita, H. Kiyoku, and Y. Sugimoto, Jpn. J. Appl. Phys., Part 2, **35**(1B), L74 (1996).
[5]F. I. Lai, S. C. Ling, C. E. Hsieh, T. H. Hsueh, H. C. Kuo, and T. C. Lu, IEEE Electron Device Lett. **30**, 496 (2009).
[6]X. A. Cao and S. D. Arthur, Appl. Phys. Lett. **85**, 3971 (2004).
[7]S. Levada, M. Meneghini, G. Meneghesso, and E. Zanoni, IEEE Trans. Device Mater. Reliab. **5**, 688 (2005).
[8]D. L. Barton, M. Osinski, C. J. Helms, N. H. Berg, and B. S. Phillips, Proc. SPIE-Int. Soc. Opt. Eng. (USA) **2693**, 64 (1996).
[9]X. A. Cao, E. B. Stokes, P. M. Sandvik, S. F. LeBoeuf, J. Kretchmer, and D. Walker, IEEE Electron Device Lett. **23**, 535 (2002).
[10]S. Keller, S. F. Chichibu, M. S. Minsky, E. Hu, U. K. Mishra, and S. P. DenBaars, J. Cryst. Growth **195**, 258 (1998).
[11]F. Scholtz, J. Off, A. Kniest, L. Görgens, and O. Ambacher, Mater. Sci. Eng., B **59**, 268 (1999).
[12]M. Meneghini, S. Podda, A. Morelli, R. Pintus, L. Trevisanello, G. Meneghesso, M. Vanzi, and E. Zanoni, Microelectron. Reliab. **46**, 1720 (2006).
[13]L. C. Chen and Y. L. Huang, Solid-State Electron. **48**, 1239 (2004).
[14]S. Bychikhin, L. K. J. Vandamme, J. Kuzmik, G. Meneghesso, and D. Pogany, ASDAM Conference Proceedings, The Fifth International Conference on Advanced Semiconductor Devices and Microsystems, Smolenice Castle, Slovakia,2004
[15]M. Sampietro, G. Ferrari, D. Natali, U. Scherf, K. O. Annan, F. P. Wenzl, and G. Leising, Appl. Phys. Lett. **78**, 3262 (2001).
[16]D. Ursutiu and B. K. Jones, Semicond. Sci. Technol. **11**, 1133 (1996).
[17]T. Mukai, S. Nagahama, M. Sano, T. Yanamoto, D. Morita, T. Mitani, Y. Narukawa, S. Yamamoto, I. Niki, M. Yamada, S. Sonobe, S. Shioji, K. Deguchi, T. Naitou, H. Tamaki, Y. Murazaki, and M. Kameshima, Phys. Status Solidi A **200**, 52 (2003).
[18]S. Leu, H. Protzmann, F. Höhnsdorf, W. Stolz, J. Steinkirchner, and E. Hufgard, J. Cryst. Growth **195**, 91 (1998).
[19]C. J. Deatcher, C. Liu, M. G. Cheong, L. M. Smith, S. Rushworth, A. Widdowson, and I. M. Watson, Chem. Vap. Deposition **10**, 187 (2004).
[20]W. K. Fong, K. K. Leung, and C. Surya, J. Cryst. Growth **298**, 239 (2007).
[21]S. Ruvimov, Z. Liliental-Weber, J. Washburn, K. J. Duxstad, E. E. Haller, Z. -F. Fan, S. N. Mohammad, W. Kim, A. E. Botchkarev, and H. Morkoç, Appl. Phys. Lett. **69**, 1556 (1996).
[22]B. P. Luther, S. E. Mohney, T. N. Jackson, M. A. Khan, Q. Chen, and J. W. Yang, MRS Symposia Proceedings No. 449 (Materials Research Society, Pittsburgh, 1997), p. 1097.
[23]R. Wenzel, G. G. Fischer, and R. Schmid-Fetzer, Mater. Sci. Semicond. Process. **4**, 357 (2001).
[24]R. Wenzel, G. G. Fischer, and R. Schmid-Fetzer, Mater. Sci. Semicond. Process. **4**, 367 (2001).
[25]M. Yoshikawa, M. Murakami, H. Ishida, and H. Harima, Appl. Phys. Lett. **94**, 131908 (2009).
[26]C. Sasaoka, H. Sunakawa, A. Kimura, M. Nido, A. Usui, and A. Sakai, J. Cryst. Growth **189–190**, 61 (1998).
[27]C. Surya, S. H. Ng, E. R. Brown, and P. A. Maki, IEEE Trans. Electron Devices **41**, 2016 (1994).
[28]M. S. Keshner, Proc. IEEE **70**(3), 212 (1982).
[29]G. Tessier, M. L. Polignano, S. Pavageau, C. Filloy, D. Fournier, F. Cerutti, and I. Mica, J. Phys. D **39**, 4159 (2006).
[30]Z. Zhang, Annu. Rev. Heat Transfer **11**, 351 (2000).

Downloaded 17 Mar 2011 to 158.132.161.180. Redistribution subject to AIP license or copyright; see http://jap.aip.org/about/rights_and_permissions